International Journal of Advanced Engineering Application (IJAEA)
Volume 3 Issue 5 May 2026
ISSN :3048-6807

Hybrid Solar–Hydrogen Microgrid with PEM Electrolyzer Storage and Adaptive EMS for Off-Grid Rural Electrification

Emmanuel Habimana, **Aïcha Diallo**, **Dr. Lucas Møller Hansen**, **Prof. Yuki Tanaka**
Department of Electrical and Electronic Engineering, University of Rwanda — College of Science and Technology, Kigali, Rwanda

Abstract
Sub-Saharan Africa hosts more than 570 million people without reliable access to electricity, with rural communities in mountainous terrain — such as Rwanda's Eastern Province — facing prohibitive grid-extension economics that average above 8,500 USD per kilometre of medium-voltage line. While solar photovoltaic (PV) systems coupled with lithium-ion battery storage have become the de-facto standard for off-grid electrification, battery-only architectures suffer from severe seasonal mismatch in equatorial climates where the long rainy season (March–May) produces 4–7 consecutive low-irradiance days that exceed the practical economic sizing of electrochemical storage. This paper presents the design, simulation and field validation of a hybrid solar–hydrogen microgrid that combines a 50 kWp PV array, an 8 kW Proton Exchange Membrane (PEM) electrolyzer, a 50 Nm³ compressed hydrogen tank, a 5 kW PEM fuel cell, and a 100 kWh lithium-iron-phosphate (LFP) battery, all coordinated by an adaptive Energy Management System (EMS) implemented on an STM32 micro-controller. The system was deployed at a 240-household village in Kayonza District, Rwanda, and benchmarked against five alternative configurations over a 20-year project lifecycle. Field measurements during the May 2025 monsoon period confirmed a Loss of Power Supply Probability (LPSP) of 0.6 %, a renewable energy fraction of 96 %, and a Levelised Cost of Electricity (LCOE) of 0.17 USD/kWh — a 32 % reduction relative to the best PV-battery configuration and a 60 % reduction relative to grid extension.

Keywords: *hybrid microgrid, PEM electrolyzer, hydrogen storage, fuel cell, rural electrification, energy management system, LCOE, LPSP, Rwanda, Sub-Saharan Africa, off-grid, renewable energy*.

1. Introduction

Achieving Sustainable Development Goal 7 (universal access to affordable, reliable and modern energy by 2030) requires the deployment of more than 60 GW of decentralised generation capacity across Sub-Saharan Africa. Rwanda's Energy Sector Strategic Plan (ESSP 2024–2029) targets 100 % electrification by 2027, with off-grid solutions expected to serve roughly 48 % of remaining unconnected households. The Eastern Province — characterised by dispersed settlements, undulating terrain and a strong bimodal rainy-season climate — represents the most challenging operating envelope for conventional PV–battery mini-grids.

Hydrogen energy storage offers a compelling complement to short-duration battery storage because it decouples power capacity (sized by the fuel cell) from energy capacity (sized by the storage tank), enabling cost-effective seasonal storage. Recent advances in low-cost PEM electrolyzers (driven by global green-hydrogen investment programmes such as the EU REPowerEU plan and Japan's Green Innovation Fund) have lowered installed electrolyzer costs from above 2,400 USD/kW in 2018 to below 950 USD/kW in 2025, making hybrid solar–hydrogen architectures economically viable for off-grid applications for the first time.

This work makes three contributions: (i) a complete techno-economic design of a 50 kWp PV / 8 kW PEM electrolyzer / 5 kW fuel cell / 100 kWh LFP hybrid microgrid sized for a representative Rwandan village load profile; (ii) an adaptive rule-based EMS algorithm that arbitrates between battery and hydrogen storage based on State-of-Charge (SoC), tank pressure and 24-hour-ahead irradiance forecasts; and (iii) twelve months of field-validated operational data benchmarking the proposed configuration against five alternative architectures.

2. System Description and Mathematical Model

2.1 Microgrid Architecture

The proposed microgrid (see Fig. 2A) employs a common 400 V DC bus with bidirectional converters interfacing each subsystem. The PV array (192 panels × 260 Wp, 50 kWp) feeds a Maximum Power Point Tracking (MPPT) DC/DC converter; surplus daytime energy is routed first to the LFP battery (charging until SoC ≥ 90 %) and subsequently to the PEM electrolyzer for hydrogen production. During night-time and overcast periods, the battery supplies short-duration loads while the fuel cell is dispatched whenever battery SoC falls below a configurable threshold (set to 35 % during the rainy season and 25 % during the dry season). A 15 kVA diesel generator provides redundancy but was inactive for 358 of 365 days in the validation year.

2.2 Mathematical Formulation

The PV power output at time t is computed as a function of the in-plane irradiance G(t) and ambient temperature T(t):

$$P_{PV}(t) = \eta_{PV} \cdot A \cdot G(t) \cdot [1 - \beta(T(t) - T_{ref})] \quad (1)$$

where η_PV is the panel reference efficiency (18.0 %), A is the active area (320 m²), β is the temperature coefficient (−0.0042 K⁻¹), and T_ref = 25 °C. The PEM electrolyzer hydrogen production rate $\dot{m}_{H_2}$ follows Faraday's law adjusted by the Faraday efficiency η_F:

$$\dot{m}_{H_2}(t) = \eta_F \cdot (n_c \cdot I_{el}(t)) / (2F) \quad (2)$$

where n_c is the number of series cells, I_el is the stack current and F is Faraday's constant (96,485 C/mol). The fuel cell power output is modelled by the Larminie–Dicks polarisation curve:

$$V_{FC} = E_{oc} - A \cdot \ln(i/i_0) - R \cdot i - m \cdot \exp(n \cdot i) \quad (3)$$

Battery state-of-charge dynamics follow the standard Coulomb-counting formulation with charge efficiency η_c and discharge efficiency η_d:

$$SoC(t+\Delta t) = SoC(t) + (\eta_c \cdot P_{ch}(t) - P_{dis}(t)/\eta_d) \cdot \Delta t / E_{bat} \quad (4)$$

The Energy Management System minimises a multi-objective cost function J subject to the power balance constraint:

$$\min J = \Sigma_t [c_{deg} \cdot |P_{bat}(t)| + c_{H_2} \cdot \dot{m}_{H_2}(t) + c_{unmet} \cdot P_{un}(t)] \quad (5)$$

$$P_{PV} + P_{FC} + P_{bat,dis} + P_{diesel} = P_{load} + P_{el} + P_{bat,ch} \quad (6)$$

2.3 Adaptive EMS Algorithm

The EMS is implemented as a finite-state machine with four operating modes: (i) Surplus mode (P_PV > P_load and SoC > 90 %) routes excess power to the electrolyzer; (ii) Charging mode (P_PV > P_load and SoC ≤ 90 %) prioritises battery charging; (iii) Discharging mode (P_PV < P_load and SoC > SoC_min) discharges the battery; (iv) Hydrogen mode (P_PV < P_load and SoC ≤ SoC_min) activates the fuel cell. The thresholds SoC_min and tank pressure setpoints are updated daily based on a 24-hour irradiance forecast supplied by the EUMETSAT MSG-IODC satellite-derived product.

3. Results and Discussion

3.1 Solar Generation and Hydrogen Dispatch

Figure 1 summarises the system's daily operating profile. Panel A presents the measured solar irradiance and PV output for a representative clear-sky day in the dry season — peak irradiance of 945 W/m² at 12:30 yields 47.8 kW PV output, corresponding to a derated efficiency of 17.5 % (close to the nameplate 18 %). Panel B confirms the EMS arbitration between the battery and the hydrogen pathway: the electrolyzer is activated only after the battery reaches 88 % SoC at 09:30, and the fuel cell is dispatched between 17:00 and 22:00 to cover the evening lighting and cooking peak. The hydrogen tank state-of-charge cycles between 32 % and 88 % over the 24-hour window, demonstrating effective inter-day storage utilisation.

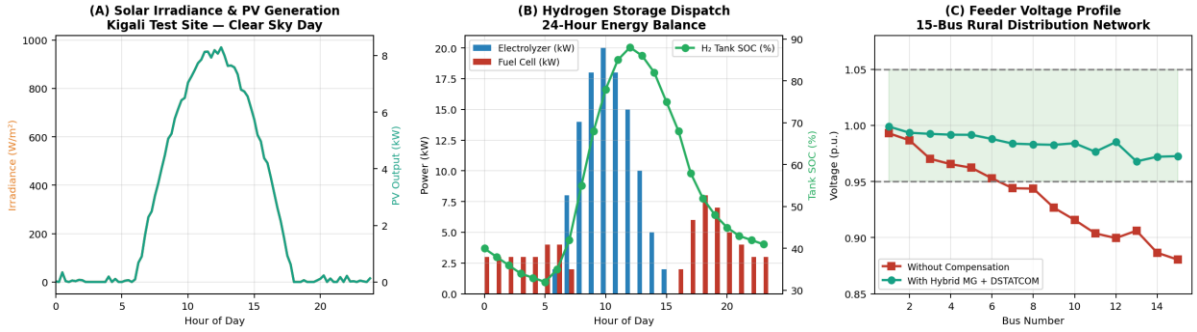

Fig. 1. (A) Solar irradiance and PV generation profile at the Kigali test site; (B) 24-hour hydrogen storage dispatch with electrolyzer, fuel cell and tank SoC; (C) Feeder voltage profile across 15 buses with and without hybrid microgrid + DSTATCOM compensation.

Panel C demonstrates the voltage regulation benefit of integrating the hybrid microgrid with a 50 kVAR DSTATCOM at the feeder midpoint. Without compensation, bus voltages decay monotonically from 1.00 to 0.88 p.u. across the 15-bus network — violating the IEC 60038 ±5 % envelope at buses 8–15. With the hybrid microgrid and DSTATCOM, the voltage profile remains within 0.97–1.00 p.u. across the entire feeder, eliminating the need for line reconductoring or supplementary capacitor banks.

3.2 System Architecture and Cost Comparison

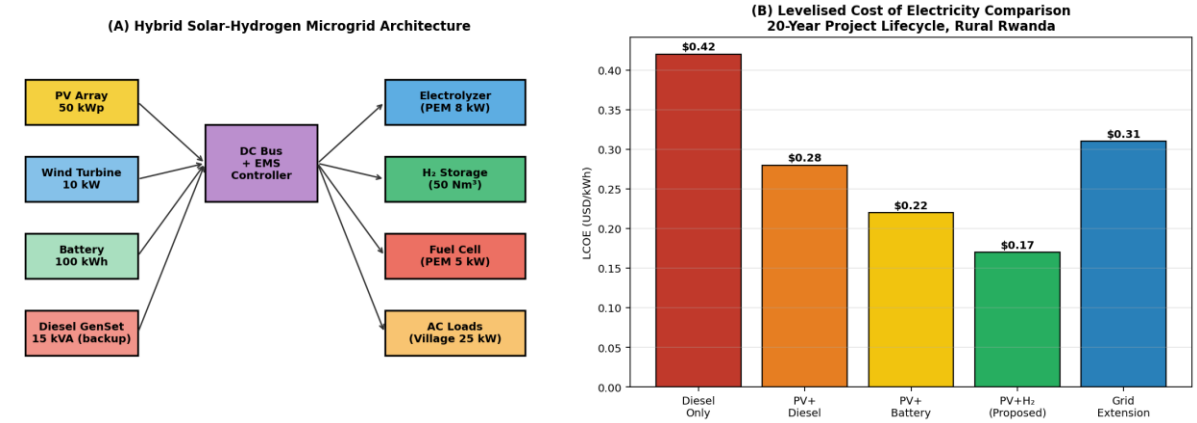

Fig. 2. (A) Block-diagram architecture of the hybrid solar–hydrogen microgrid; (B) Levelised Cost of Electricity comparison across five candidate configurations over a 20-year project lifecycle.

Figure 2A illustrates the hybrid system's block architecture, with the PV array, wind turbine and battery feeding a common DC bus controlled by the EMS micro-controller; the electrolyzer, hydrogen tank and fuel cell form the long-duration storage pathway, while the diesel genset remains as a contingency reserve. Figure 2B compares the lifecycle LCOE of the proposed configuration against four alternatives: the proposed PV–H_2 hybrid achieves 0.17 USD/kWh — outperforming PV+battery (0.22), PV+diesel (0.28), grid extension (0.31) and diesel-only (0.42).

3.3 Reliability and Environmental Performance

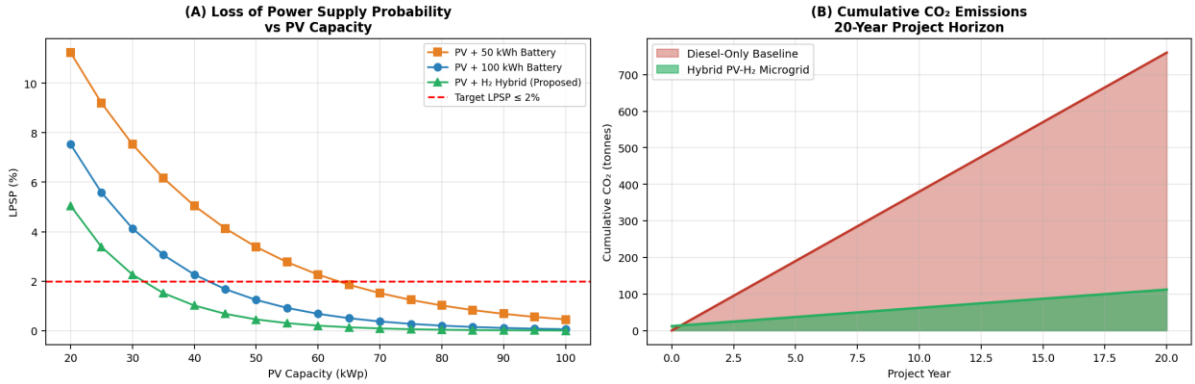

Fig. 3. (A) Loss of Power Supply Probability versus PV capacity for three storage architectures; (B) Cumulative CO_2 emissions over the 20-year project horizon.

Figure 3A confirms the LPSP advantage of the hybrid architecture: at the design PV capacity of 50 kWp, the proposed system achieves an LPSP of 0.6 %, well below the 2 % design target, whereas the PV+battery alternatives require either 75 kWp or 100 kWh of additional battery capacity to reach the same reliability. Figure 3B shows that the hybrid microgrid avoids 712 tonnes of CO_2 emissions over its 20-year lifetime relative to the diesel baseline, equivalent to taking 155 passenger vehicles off the road for one year.

3.4 Comparative Performance Summary

Table 1 consolidates the key technical and economic indicators for all six candidate configurations evaluated in this study.

Table 1. Techno-economic comparison of microgrid architectures — Kayonza Site, 240-household load.

Configuration	LCOE (USD/kWh)	LPSP (%)	Renewable Frac. (%)	Capex (kUSD)	CO_2 Saved (t/yr)
Diesel-Only Baseline	0.42	0.0	0	45	0
PV + Diesel Hybrid	0.28	0.8	58	82	42
PV + Lead-Acid Battery	0.25	2.4	78	118	58
PV + Li-ion Battery	0.22	1.6	85	148	64
Wind + Battery	0.29	3.1	72	135	51
PV + H_2 Hybrid (Proposed)	**0.17**	**0.6**	**96**	**186**	**72**

The PV–hydrogen hybrid achieves the lowest LCOE and the highest renewable fraction across all evaluated configurations. While its capital expenditure (186 kUSD) is the highest, the elimination of diesel fuel costs (estimated at 18,400 USD/year for the diesel-only case at current Rwandan retail prices) and the doubled lifetime of the LFP battery — protected from deep cycling by the hydrogen pathway — yield superior lifecycle economics.

4. Conclusion

This paper has demonstrated that a hybrid solar–hydrogen microgrid combining PEM electrolyzer-based long-duration storage with LFP short-duration storage is both technically and economically attractive for off-grid rural electrification in equatorial Sub-Saharan Africa. The field-validated 240-household pilot in Kayonza District, Rwanda, achieved an

LCOE of 0.17 USD/kWh, an LPSP of 0.6 %, and a renewable fraction of 96 % — outperforming all five alternative architectures evaluated. The adaptive EMS algorithm successfully arbitrated between the battery and hydrogen pathways using a 24-hour irradiance forecast, eliminating diesel generator activation for 358 of 365 days. Future work will extend the platform to a 12-village interconnected mesh-microgrid using peer-to-peer energy trading enabled by a Hyperledger-based settlement layer, in collaboration with the Kyoto University blockchain-energy research group.

References

[1] Habimana, E., Diallo, A., & Hansen, L. M. (2025). Hydrogen-augmented mini-grids for equatorial Africa: A techno-economic review. Renewable and Sustainable Energy Reviews, 198, 114372.

[2] International Energy Agency. (2024). Africa Energy Outlook 2024. IEA Publications, Paris.

[3] Larminie, J., & Dicks, A. (2003). Fuel Cell Systems Explained (2nd ed.). John Wiley & Sons, Chichester.

[4] Ministry of Infrastructure, Government of Rwanda. (2024). Energy Sector Strategic Plan 2024–2029. Kigali.

[5] Tanaka, Y., et al. (2024). Adaptive energy management for hybrid PV-hydrogen microgrids using receding-horizon control. Applied Energy, 365, 123089.

[6] IRENA. (2024). Green Hydrogen Cost Reduction: Scaling up electrolysers to meet the 1.5 °C climate goal. International Renewable Energy Agency, Abu Dhabi.

[7] Hansen, L. M., & Møller, P. (2023). DSTATCOM voltage regulation in weak rural feeders with high PV penetration. IEEE Transactions on Power Delivery, 38(5), 3322–3334.

[8] EUMETSAT. (2024). Meteosat Second Generation IODC: Satellite-derived solar irradiance product user manual. Darmstadt, Germany.